HHS Public Access

Author manuscript

Cell Metab. Author manuscript; available in PMC 2019 August 01.

Published in final edited form as:

Cell Metab. 2016 December 13; 24(6): 835–847. doi:10.1016/j.cmet.2016.10.005.

Browning of White Adipose Tissue with Roscovitine Induces a Distinct Population of UCP1+ Adipocytes

Hong Wang[1], **Libin Liu**[1], **Jean Z. Lin**[1], **Tamar R. Aprahamian**[2], **Stephen R. Farmer**[1,3,*]

[1]Department of Biochemistry, Boston University School of Medicine, Boston, MA 02118, USA

[2]Renal Section, Department of Medicine, Boston University School of Medicine, Boston, MA 02118, USA

SUMMARY

Brown-like adipocytes exist in several adipose depots including white (WAT) as well as brown (BAT). Activation of these UCP1$^+$ cells is a potential therapeutic strategy to combat obesity. Studies have shown that posttranslational modifications of PPARγ regulate select adipocyte programs. Deacetylation of K268 and K293 in the ligand-binding domain of PPARγ by Sirt1 induces browning of WAT. Phosphorylation of S273 of PPARγ by CDK5 or ERK stimulates a diabetogenic program of gene expression in WAT. Here, we report that roscovitine, a CDK inhibitor, prevents S273 phosphorylation and promotes formation of UCP1$^+$ (brite) adipocytes in WAT. It also enhances energy expenditure as well as prevents diet-induced obesity and insulin resistance. Analysis of fluorescence-activated cell-sorted UCP1$^+$ adipocytes shows that the mRNA signature of brite adipocytes is distinct from beige adipocytes, which arise through catecholamine signaling. These results suggest that brown-like adipocytes in WAT may arise from multiple origins.

Graphical abstract

*Correspondence: sfarmer@bu.edu.
[3]Lead Contact

ACCESSION NUMBERS

The accession number for the microarray data reported in this paper is GEO: GSE87191.

SUPPLEMENTAL INFORMATION

Supplemental Information includes Supplemental Experimental Procedures and four figures and can be found with this article online at http://dx.doi.org/10.1016/j.cmet.2016.10.005.

AUTHOR CONTRIBUTIONS

S.R.F. and H.W. conceived the study and designed experiments. H.W., L.L., and J.Z.L. performed experiments and analyzed data. T.R.A. generated the UCP1-Cre:mTmG mouse. S.R.F. and H.W. wrote the manuscript. H.W., L.L., J.Z.L., and T.R.A. edited the manuscript.

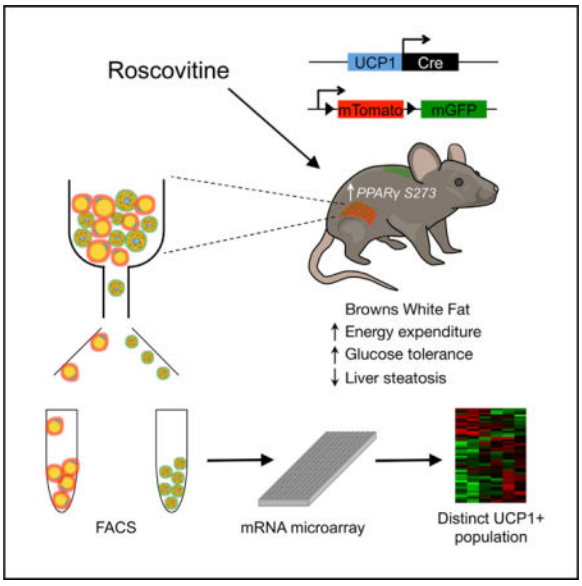

INTRODUCTION

Adipose tissue exists within multiple anatomical locations where it functions to control energy expenditure as well as regulate many metabolic processes. Excess storage of triglycerides (TGs) and other lipids in specific depots, most notably those surrounding the internal organs (visceral depots), can lead to insulin resistance, dyslipidemia, fibrosis, and cancer. The various depots are composed of an array of cell types including adipocytes as well as many others that contribute to the multifaceted function of each depot (Cinti, 2005, 2012). Adipocytes are generally classified as white and brown, the former storing TGs and the latter utilizing lipids to produce heat. White adipocytes deposit TGs in a single large lipid droplet (unilocular) that occupies a majority of the cytoplasm. Brown adipocytes have multiple lipid droplets (multilocular) and many mitochondria that contain a unique uncoupling protein (UCP1) to uncouple electron transport from the generation of ATP for heat production (Cannon and Nedergaard, 2004). All adipocytes secrete a plethora of factors and hormones that act locally or enter the circulation to contribute to systemic endocrine actions (Deng and Scherer, 2010). Various depots can undergo extensive remodeling as the organism adapts to energy demands, to stress (i.e., cold) and other responses to maintain metabolic homeostasis (Sun et al., 2011). One prominent remodeling process is recruitment of brown-like adipocytes to white adipose tissue (WAT) in response to a variety of physiological as well as pharmacological effectors (Giordano et al., 2014). These cells contain multiple lipid droplets and express thermogenic genes including UCP1. They also express genes that are considered markers of white adipocytes at levels significantly lower than in visceral white depots (Vernochet et al., 2009). The appearance of these brown-like cells in WAT has been observed in many investigations over the last three decades, but interest in their potential physiological function has only recently been revisited. This primarily is due to the identification of thermogenic tissues in adult humans, which have characteristics similar to the brown-like tissue interspersed within mouse WAT and activation of this tissue is a potential antiobesity therapy (Farmer, 2009).

The brown-like cells recruited to WAT through cold exposure arise from progenitors expressing TMEM26 and CD137 on their cell surface and are referred to as beige adipocytes (Wu et al., 2012). A percentage of these beige cells are derived from smooth muscle-like cells that once expressed myosin heavy chain 11 (Myh11). Other brown-like cells can be recruited to WAT following exposure to PPARγ ligands (Qiang et al., 2012; Vernochet et al., 2009). These cells are often referred to as brite adipocytes (Petrovic et al., 2010). The origin of these cells is not known. It is possible they are identical to beige cells and stem from the same source of progenitors even though the action of the respective inducers is distinct. Cold stimulates a β-adrenergic pathway compared to activation of PPARγ. In this regard, it has been suggested that brite cells arise through transdifferentiation of pre-existing white adipocytes (Giordano et al., 2014).

We previously showed that treatment of mice with a potent PPARγ ligand induced expression of brown genes in WAT including UCP1, cidea, and FGF21 but also suppressed many visceral white genes including angiotensinogen and chemerin (Vernochet et al., 2009). Transcription of many target genes by PPARγ was shown to require repositioning helix 12 to facilitate association of coactivators in response to ligand binding (Nolte et al., 1998). Studies by our group and others further demonstrated that regions of the ligand-binding domain other than helix 12 also influenced ligand activity (Liu et al., 2006; Pascual et al., 2005; Wang et al., 2008). In particular, F372 within helix 7 was shown to be important for the ligand-dependent in vitro induction of brown genes as well as suppression of the white genes (Wang et al., 2008). Qiang et al. (2012) later showed that deacetylation of K268 and K293 in helix 2/3 of PPARγ by Sirt1 is capable of browning WAT and protects mice from diet-induced obesity and insulin resistance. Studies by Spiegelman and colleagues have shown that phosphorylation of S273 of PPARγ by CDK5 or ERK stimulates a diabetogenic program of gene expression (Banks et al., 2015; Choi et al., 2010, 2011). Pharmacological inhibition of MEK/ERK prevents S273 phosphorylation, suppresses the diabetogenic genes, and improves insulin resistance in obese mice (Banks et al., 2015).

Because S273 is flanked by K268 and K293, we questioned whether phosphorylation of S273 also regulates browning of WAT. We show that treatment of mice with a CDK inhibitor, roscovitine, browns inguinal WAT (iWAT) to the same extent as rosiglitazone treatment. Profiling of RNA from UCP1-positive adipocytes isolated by fluorescence-activated cell sorting (FACS) from iWAT of mice treated with a β-adrenergic agonist, CL316,243 (CL), rosiglitazone (RG), or roscovitine (RS) identifies two distinct populations of brown-like cells. Beige (CL316,243) and classic brown adipocytes are closely related, while rosiglitazone and roscovitine cells are similar and distinct from the others. All cells express UCP1 along with most of the genes associated with thermogenesis and mitochondrial activity. The mechanism of browning is consistent with roscovitine preventing the phosphorylation of S273 of PPARγ. Taken together, the data show different mechanisms of browning WAT give rise to distinct populations of $UCP1^+$ cells suggesting that brown-like adipocytes may arise from multiple origins.

RESULTS

K268 and K293 of PPARγ can be posttranslationally modified to regulate browning of WAT. S273 is flanked by these lysines, and when phosphorylated by CDK5 and/or ERK, the insulin-sensitizing activity of PPARγ in adipocytes is significantly attenuated. We hypothesized that inhibition of S273 phosphorylation would mimic effects of deacetylation of K268 and K293 by inducing brown gene expression. Treatment of 3T3-L1 adipocytes with roscovitine, a CDK inhibitor, for 1–2 days induced select brown adipocyte mRNAs including PRDM16, PGC-1α, FGF21, and UCP1 (Figure 1A) and UCP1 protein (Figure 1C) without altering expression of standard adipogenic genes such as adiponectin and FABP4 (Figure 1B). The drug was shown to be an effective inhibitor of S273 phosphorylation in the mature cells (Figure 1D). To investigate whether S273 phosphorylation/dephosphorylation of PPARγ determines the browning activity of roscovitine, Swiss 3T3 cell lines expressing wild-type and S273A forms of PPARγ were generated. The TNFα-associated phosphorylation of S273 of PPARγ in WT cells could be blocked by roscovitine (Figure S1A), and, of course, PPARγ could not be phosphorylated at S273 in the mutant cell line (Figure 1E). These Swiss cell lines undergo extensive and similar degrees of adipogenesis when stimulated with a standard hormonal cocktail consisting of dexamethasone, methyl-isobutylxanthine, and insulin (Figure S1B). It was not necessary to include a thiazolidinedione (TZD), as is the case with many other fibroblast lines. qPCR analysis of mRNAs showed equivalent expression of FABP4 and adiponectin in each cell line consistent with equivalent adipogenesis (Figure 1F). The S273A cells, however, had enhanced levels of brown adipocyte mRNAs including PRDM16 and UCP1 (Figure 1F). Earlier studies by our group and others have shown that TZDs can also induce brown gene expression in white adipocytes (Petrovic et al., 2010; Vernochet et al., 2009). We questioned, therefore, whether the action of TZD is independent of S273 phosphorylation status. Figure 1G shows that TZD induces UCP1 protein expression to about the same extent in WT and S273A cells, which is to a similar level reached through expression of S273A PPARγ alone. In fact, earlier studies by Spiegelman and coworkers suggested that the anti-diabetogenic action of TZDs is, in part, through the inhibition of S273 phosphorylation (Choi et al., 2010). We also questioned whether the browning activity of roscovitine is through inhibition of S273 phosphorylation. The data in Figure 1H demonstrates that roscovitine induces brown genes in WT Swiss-PPARγ cells to the same extent as S273-PPARγ cells alone, and addition of the drug to S273 cells had no additional browning activity. To determine whether the browning activity of roscovitine involved selective interaction of PPARγ with brown gene promoters and cofactors, we performed two analyses. First, we demonstrate using ChIP-qPCR that both roscovitine as well as S273A enhances the binding of PPARγ to the promoters of *Pgc1a, Ucp1*, and *Fgf21* genes with no effect on binding to white gene promoters such as *retn* and *pank3* (Figure 1I). Second, we immunoprecipitated a MYC-tagged PPARγ from cells treated with or without roscovitine and show the drug promotes the interaction of PPARγ with PRDM16 and Sirt1 and dissociates its interaction with NCoR1 (Figure 1J). Importantly, we show that treatment of mice with roscovitine (RS) for 2 weeks induces expression of UCP1 in iWAT to the same extent as treatment with CL316,243 (CL) or rosiglitazone (RG), whereas browning only occurs in eWAT in response to CL (Figure 1K). Consistent with the in vitro studies, roscovitine prevented the phosphorylation of S273 as well as S112 of

PPARγ in both iWAT and eWAT while potently activating MEK/ERK as shown previously by others (Banks et al., 2015).

Roscovitine Browns White Adipose Tissue and Enhances Energy Expenditure

These studies strongly support the notion that roscovitine is stimulating the browning activity of PPARγ. Studies by Qiang et al. (2012) previously showed that deacetylation of PPARγ in mice not only induced browning but also regulates energy homeostasis by promoting energy expenditure over storage. To determine whether roscovitine-induced browning also affects energy balance, mice were given roscovitine, CL316,243, or rosiglitazone every day for 6 weeks at which various physiological parameters were measured. Immunohistochemical staining of adipose tissue for UCP1 shows that all three agents induced extensive browning of iWAT (Figure 2A) with minimal browning of eWAT (Figure S2A). Western blot analysis also showed that the extent of UCP1 expression in iWAT is similar for all three treatments (Figure 2B). Fat mass was significantly lower in mice treated with roscovitine and CL316,243 compared to control and rosiglitazone-treated mice (Figure 2C). Moreover, individual adipocytes were smaller in the eWAT depot of mice given roscovitine and CL316,243 (Figure S2A). In all cases, food intake, lean mass, and physical activity were the same for the three agents and did not differ from control values (Figures 2D–2F). Furthermore, all drug-treated mice exhibited enhanced glucose tolerance with CL316,243 being the most potent enhancer (Figure 2G). Only roscovitine and CL316,243 suppressed circulating levels of insulin (Figure S2B). The extensive decrease in fat mass without a change in food intake or lean mass suggested that roscovitine and CL316,243 were enhancing energy expenditure. In fact, analysis of all treated mice in Comprehensive Laboratory Animal Monitoring System (CLAMS) metabolic cages showed an increase in VCO_2 and VO_2 (Figures 2H and 2I) in response to roscovitine and CL316,243. Rosiglitazone did not increase energy expenditure. The RER values for all agents were the same and were consistent with metabolism of a carbohydrate-enriched diet (Figure S2C). Importantly, the morphology of BAT and its expression of UCP1 was not altered by any of the drugs (Figures 2J and 2K) supporting the notion that roscovitine enhances energy expenditure in a BAT-independent manner.

Roscovitine Protects against Diet-Induced Obesity and Insulin Resistance

Next, we questioned whether roscovitine alters the metabolic response to a high fat diet (HFD). Mice were given a HFD for 9 weeks and treated with roscovitine, rosiglitazone, or CL316,243 every day during the last 6 weeks of the diet. Roscovitine suppressed weight gain (Figure 3A) and fat mass (Figure 3B) to a greater extent than the other two drugs without any change in lean mass or food intake (Figures 3C and 3D). The HFD resulted in hypertrophy of individual adipocytes in iWAT of control and rosiglitazone-treated mice, but this was dramatically reduced in response to roscovitine and CL316,243 (Figure 3E). All three drugs protected mice from diet-induced inflammation as observed by a corresponding loss of crown-like structures in eWAT (Figure 3E). Similarly, all three drugs protected against diet-induced glucose intolerance and reduced circulating levels of insulin (Figures 3F and 3G). Morphological analysis of the liver demonstrated that the HFD caused steatosis, which was only eliminated by treatment with roscovitine (Figure 3H). Rosiglitazone

appeared to enhance the deposition of lipids in the liver as reported by others (Rull et al., 2014).

There is little known about the phenotype of UCP1$^+$ adipocytes residing in WAT following treatment of mice with different browning agents. Spiegelman and coworkers have identified the origin of UCP1$^+$ cells arising in response to cold exposure and referred to them as beige adipocytes (Wu et al., 2012). These cells express gene signatures that reflect the host white tissue as well as smooth muscle like genes (Long et al., 2014). To identify the phenotype of the brown-like adipocytes induced by roscovitine, rosiglitazone, or CL316,243, we generated mice in which UCP1$^+$ adipocytes express GFP, while all other cells including white adipocytes express RFP. Figure S3 shows that the BAT depot emits an intense green fluorescence while the surrounding white adipose is red in mTmG mice expressing UCP1-Cre. Visualization of whole mounts of adipose tissue from these mice (Figure 4A) shows the presence of small GFP$^+$ cells within the iWAT depot following treatment with CL316,243 (CL+Cre), roscovitine (RS+Cre), as well as rosiglitazone (RG+Cre). iWAT from untreated mice (+Cre) (Figure 4A) as well as control mice lacking the UCP1-cre transgene (data not shown) have undetectable levels of GFP fluorescence. To visualize individual adipocytes, the respective tissues were digested with collagenase, and total adipocytes floated to the surface while stromal vascular cells pelleted following a low speed centrifugation. The adipocytes were collected and visualized by fluorescence confocal microscopy. The white adipocytes contain an outer rim of intense red fluorescence corresponding to the membrane tethered tomato protein (RFP) surrounding a large single lipid droplet. The UCP1$^+$ cells corresponding to CL316,243 treatment had a green fluorescent rim (GFP) surrounding multiple lipid droplets. Surprisingly, virtually all of the roscovitine-induced UCP1$^+$ adipocytes had a green rim around a single or few lipid droplets (Figure 4B). This morphology has been termed paucilocular by Giordano et al. (2014).

The recruitment of UCP1$^+$ adipocytes in response to roscovitine could occur through many physiological mechanisms. Induction of beige adipocytes by cold is considered to involve release of catecholamines through direct and indirect (sympathetic nervous system) means. CL316,243, being a potent β-adrenergic agonist, acts in a manner similar to catecholamines and, therefore, mimics cold exposure and produces beige cells (Wu et al., 2012). Rosiglitazone through its activation of PPARγ has been suggested to stimulate the brown gene program in pre-existing preadipocytes or mature adipocytes. The resulting UCP1$^+$ cells have been referred to as brite adipocytes (Petrovic et al., 2010). To obtain mRNA signatures of each population of UCP1$^+$ adipocytes from WAT, it was necessary to isolate the brown-like cells from the surrounding white cells. To do this, we established a cell isolation procedure in which the adipocyte fraction of collagenase digested adipose tissue of UCP1+Cre mice was subjected to fluorescence-activated cell sorting as outlined in the Experimental Procedures. Figure 4C shows that GFP-fluorescing (UCP1$^+$) cells (Drugs +Cre) can be successfully sorted from RFP cells, which consist predominantly of white adipocytes (Saline+Cre) because stromal vascular cells have been removed prior to sorting. To gain insight into the gene expression signatures of all UCP1$^+$ adipocytes, GFP-positive cells were collected by FACS from iWAT of mice treated with CL316,243, rosiglitazone, or roscovitine. BAT UCP1$^+$ cells as well as white adipocytes were also harvested from untreated mice. qPCR analysis of RNA isolated from all five populations of cells shows

similar levels of common adipogenic markers including perilipin, adipsin, adiponectin, and aP2 (FABP4) (Figure 4D). The four populations of UCP1$^+$ adipocytes, (BAT, CL, RS, and RG), expressed elevated amounts of the common brown genes including UCP1, Otop1, PGC1α, Cidea, Elovl3, Cox7a, and Acot11. The RS and RG cells, however, expressed several of these brown markers at levels several fold lower than BAT or CL adipocytes as shown, particularly for UCP1, Cox7a, and Acot11 (Figure 4E).

Roscovitine Induces Formation of a Unique Population of UCP1$^+$ Adipocytes

To compare the gene signatures of the different cell types, the five RNA samples analyzed in Figure 4 (WAT, BAT, CL, RS, and RG) were amplified and subjected to microarray analysis (Figure 5). At a global level, the signatures of all five adipocyte types were very similar as revealed through pairwise comparisons of each of the samples (Figure S4). In fact, a majority (>95%) of RNA sequences are common to all UCP1$^+$ adipocytes including BAT as well as white adipocytes. Heatmaps were created of all the genes that had an absolute value fold change >2 (Figure 5A). It is very clear that the five signatures are different suggesting that the UCP1$^+$ adipocytes are distinct from each other. As an additional approach, principal component analysis was performed using all 25,000 probe sets across the five samples. These results show that of the UCP1$^+$ adipocyte transcriptomes, the CL316,243 signature is closest to that of BAT. The signatures of roscovitine (RS) and rosiglitazone (RG) cells are very similar but distinct from that of WAT, BAT, and CL adipocytes (Figure 5B).

To identify potential gene markers for each of the adipocyte types, we analyzed the transcriptomes and selected genes whose expression differed 3-fold or greater between the cell types. The Venn diagram of the overlapping genes enriched in classical brown adipocytes and beige/brite adipocytes versus white adipocytes (Figure 5C) shows that there are relatively few mRNAs that can be considered to be cell-type-specific. These few genes are presented in the heatmap shown in Figure 5D and some were selected as potential markers for each cell type. To validate these selections, we analyzed cell type marker expression in RNA isolated from each of the FACS samples by qPCR assays. Some genes including Magea1, Nlrp9c, Tdpoz2, Slc22a29, Camsap3, and Kng2 are more highly expressed in BAT cells compared to the other UCP1$^+$ adipocytes and can be considered to be BAT-selective (Figure 5E). We also found that Arhgdig is expressed predominantly in BAT in agreement with Long et al. (2014). Adcy3, Khdrbs3, Phospho1, Ppp1r3b, and Tmem79 are expressed primarily in BAT and CL316,243 cells compared to all other cells (Figure 5F). CL-selective genes include Pcdha3, Scd3, and Trim17 (Figure 5G) while Cdsn, Rhbg, and Gpx8 are most abundant in brite (RS and RG) adipocytes (Figure 5I). Examples of genes that distinguish RS from RG cells are Tas2r108 (RG-selective) and Sec31b (RS-selective) (Figure 5H).

The brite adipocytes (RS and RG) are clearly different from beige cells (CL) both at the level of morphology and mRNA signatures. It is conceivable, however, that each population arise from the same progenitors, and the brite cells are at an earlier stage of differentiation than the beige cells. To test this possibility, we generated two populations of UCP1$^+$ adipocytes: immature beige cells by treating mice with CL316,243 for only 3 days and mature brite cells by giving roscovitine for 10 days. Figure 6A shows that the immature

beige cells have multiple lipid droplets and are significantly smaller than the corresponding mature cells after 7 days of CL treatment. They are also significantly different from the mature brite cells, which are large, paucilocular cells (Figure 6A, RS+10d). To further characterize these UCP1$^+$ cells, we analyzed expression of select mRNAs in 3-day beige (CL) and 10-day brite (RS) cells following their isolation by FACS as described in Figure 4. Figure 6B shows that both immature beige (CL) and mature brite cells (RS) express levels of UCP1 and Acot11 mRNAs many times lower than classic brown adipocytes (BAT). Interestingly, the immature beige cells (CL) are capable of expressing the CL-specific marker, Trim17, many fold higher than BAT and mature brite (RS) cells. Similarly, the RS cells express four of the brite markers (RS or RG), Gpx8, Rhbg, Cdsn, and Sec31b at levels significantly higher than all other cells (CL, BAT, or WAT). These data strongly suggest that brite cells are not immature beige cells. We also questioned whether the low level of Ucp1 and Acot11 mRNAs in mature brite cells (Figure 4E) is due to the absence of a thermogenic stimulus in the corresponding mice. (The mature beige cells, of course, express Ucp1 because they constantly receive β-adrenergic stimulation due to the daily injection of mice with CL316,243 for 7 days). To address this question, we generated mature brite cells in mice by a 10-day treatment with roscovitine and stimulated them with CL316,243 for 3 days (R+C in Figure 6B). qPCR analysis was then performed on RNA from FACS UCP1$^+$ cells as in Figure 5. It is important to emphasize that this population of UCP1$^+$ cells (R+C) will contain both mature brite as well as immature beige cells. It is interesting, therefore, that the levels of UCP1 and Acot11 mRNAs are many fold higher in the mixed sample (R+C) than in brite (RS) or beige (CL) cells, which were separately analyzed. As expected, the BAT-specific Kng2 was not induced by CL in the brite cells. A comparison of the relative levels of the CL marker (Trim17) with the RS markers (Gpx8, Rhbg, Cdsn, Sec31b) shows that the mixed population of UCP1$^+$ cells (R+C) contains significantly more RS than CL cells. Taken together, these data show that brite cells (RS) express lower levels of UCP1 as well as Acot11 mRNAs because they are not receiving an adequate thermogenic stimulus, but once this stimulus is given (CL), these mRNAs are induced in the mature RS cell. The fact that CL cells represent a significantly smaller fraction of the mixed R+C population confirms that induction of UCP1 and Acot11 mRNAs by CL occurs in pre-existing RS cells.

To demonstrate the functionality of the different UCP1$^+$ adipocytes, we assessed the response of mice treated with the browning agents to cold exposure. Mice were pretreated with CL, RS, or RG for 10 days at room temperature then moved to the cold room (4°C) for 3 days. Rectal temperature was measured at outset and every 24 hr. Figure 6C shows that mice given the drugs each had higher starting temperatures than control untreated mice with CL being the highest. The temperature of mice with brite (RS and RG) and beige (CL) adipocytes dropped slightly during the 72-hr cold exposure but not as dramatically as it did in control mice. The western blot shown in Figure 6D demonstrates that the response to cold correlated with the level of expression of UCP1 in iWAT. Mice treated with the three drugs express UCP1 at higher levels than untreated mice consistent with their higher body temperatures. Importantly, exposure to cold induced UCP1 expression in the pretreated mice many fold higher than cold exposure in untreated mice. These data show that the pre-existing brite adipocytes respond to a thermogenic stimulus and, in doing so, defend the body temperature against cold.

DISCUSSION

In this report, we present a mouse model that facilitates a detailed molecular analysis of UCP1$^+$ adipocytes arising in white adipose tissue of mice treated with different browning agents. Roscovitine and rosiglitazone produce UCP1$^+$ cells that have gene expression signatures distinct from the signature of beige adipocytes (CL316,243-induced cells). We show that roscovitine enhances energy expenditure and protects mice from diet-induced obesity and glucose intolerance. Rosiglitazone has no effect on energy balance and only protects against diet-induced glucose intolerance. We further demonstrate that roscovitine-induced browning occurs through mechanisms that are consistent with it blocking the phosphorylation of PPARγ at sites previously shown to regulate insulin sensitivity (Choi et al., 2010).

Our ability to obtain highly enriched populations of adipocytes from mice treated with different browning agents has provided strong evidence for additional types of UCP1$^+$ adipocytes besides classical brown and beige cells. Previous classification of these cells is based primarily on gene signatures obtained through analysis (microarray and deep sequencing) of RNA isolated from adipose tissues. A detailed molecular description of beige and brite adipocytes was not possible because the cells reside within a complex environment of multiple other cell types including white adipocytes, preadipocytes, vascular, and immune cells. To overcome this problem, Spiegelman and coworkers (Long et al., 2014) applied translating ribosome affinity purification (TRAP) technology to selectively isolate polysomes of UCP1$^+$ cells directly from whole adipose tissue of mice. Analysis of the RNAs contained on the polysomes revealed interesting signatures of UCP1$^+$ adipocytes present in different white depots. Most notably, their analysis detected a smooth muscle (SM) gene expression signature in beige cells but not classical brown adipocytes, which led them to show that a small percentage of beige cells arise from smooth muscle like cells that express Myh11. The TRAP approach, however, did not detect Tmem26 preferentially in beige cells or Zic1 in brown cells, two markers that have been used by many to assign tissue-type identity. Long et al. (2014) suggested that a limitation of the TRAP approach is that actively translating mRNAs may not completely reflect total mRNAs in beige or brown cells. Employing a method that selectively sorts UCP1$^+$ adipocytes from all other cells in the brown and white depot has allowed us to obtain gene signatures corresponding to the total mRNA population of each of the adipocyte types.

As stated above, the most important outcome of our strategy was to provide evidence for existence of different types of UCP1$^+$ adipocytes forming in the subcutaneous white depot in response to different browning agents. Roscovitine, rosiglitazone, and CL316,243 produce UCP1$^+$ adipocytes that express a common signature of mRNA coding for proteins involved in mitochondrial functions and adaptive thermogenesis. There are many differences, however, between each of the cell types, suggesting that they might arise from diverse origins. The analysis has also identified several genes that are enriched in each cell type that have not previously been associated with UCP1$^+$ adipocytes and can now be used as a novel set of markers for future classification of each cell type. For example, Cdsn, Rhbg, and Gp×8 are much more highly expressed in brite cells (roscovitine and rosiglitazone) than in other cell types. Pcdha3, Scd3, and Trim17 are selectively expressed in beige cells while

Magea1, Nlrp9c, Tdpoz2, Slc22a29, Camsap3, and Kng2 are primarily expressed in BAT. Trim17 is beige cell (CL)-specific. Another interesting and important observation is the significant difference in morphology of brite adipocytes compared to beige cells. The former are paucilocular, while the latter are multilocular.

We did consider whether brite adipocytes are simply immature beige cells that have not reached maturity due to the absence of a β-adrenergic stimulus, which drives beige adipogenesis. The data show, however, that immature beige adipocytes are different from mature brite cells based on their different patterns of select gene expression (Figure 6). Additionally, immature beige cells have an identical overall morphology as their mature counterparts (multilocular) except are much smaller in size (data not shown). In contrast, the mature brite cells are primarily paucilocular containing few lipid droplets and, in some cases, only a single large droplet. Gene expression analysis shows that despite their morphological similarity to white cells, they have a distinct mRNA signature. We also questioned why expression of UCP1 and other brown genes is so low in brite cells and reasoned that the cells are not receiving a thermogenic stimulus. We demonstrate that this is the case because addition of CL316,243 to mice already containing abundant numbers of brite cells in iWAT induces UCP1 expression in these cells to levels approaching those in the BAT depot. It is important to mention that the brite cells still maintain their distinct phenotype following the β-adrenergic stimulus (i.e., abundant expression of Gp×8, Rhbg, Cdsn, and Sec31b).

The data in Figure 1 suggests that roscovitine induces browning by selectively stimulating PPARγ through the inhibition of phosphorylation of S112 and S273. To support this notion, we show that expression of S273A PPARγ in Swiss 3T3 cells induces brown adipocyte genes. The importance of S273 in bestowing insulin-sensitizing activity on PPARγ was originally shown by Spiegelman and coworkers (Choi et al., 2010). They demonstrated that S273 is phosphorylated in inflamed adipose tissue, which leads to attenuation of gene expression associated with systemic insulin action including adiponectin and adipsin genes. Their in vitro studies demonstrated that CDK5 phosphorylates S273, which could be blocked by agonist and non-agonist ligands of PPARγ including rosiglitazone. However, mice deficient in CDK5 are insulin-resistant rather than the expected insulin-sensitive. This turned out to be due to activation of ERK because CDK5 phosphorylates and attenuates the activity of MEK1. Furthermore, it was shown that ERK also phosphorylates S273 as well as S112: two events that inhibit PPARγ activity. It was subsequently shown that treatment of mice with an ERK inhibitor improves insulin-resistance in obese wild-type (WT) and ob/ob mice (Banks et al., 2015). Figure 1K shows that roscovitine inhibited phosphorylation of S273 and S112 as well as activated the MEK/ERK pathway in adipose tissue. One interpretation is that roscovitine inhibits CDK5 activity and somehow prevents ERK from phosphorylating PPARγ. The resulting unphosphorylated PPARγ can then induce the formation of $UCP1^+$ adipocytes (brite) in the iWAT depot. It is also important to point out the close similarity of mRNA signatures of roscovitine- and rosiglitazone-derived $UCP1^+$ adipocytes (Figure 5). This provides additional support for the idea that roscovitine browns WAT, in part, by selectively activating PPARγ.

UCP1$^+$ adipocytes recruited to WAT in response to cold or CL316,243 treatment (beige) arise from progenitors expressing TMEM26 and CD137 as well as smooth muscle-like markers (Long et al., 2014; Wu et al., 2012). The precise origin of the brite adipocytes arising due to activation of PPARγ(rosiglitazone and roscovitine), however, is not known. It has been proposed that brite cells arise through transdifferentiation of white adipocytes (Giordano et al., 2014). The fact that rosiglitazone can induce brown gene expression in white adipocytes in culture supports this notion (Vernochet et al., 2009). It is also possible that activation of PPARγ redirects the normal differentiation of white preadipocytes to brown adipocytes. PPARγ, however, is expressed in other cell types besides preadipocytes and adipocytes. Studies by Graff and colleagues show that PPARγ$^+$ progenitors are essential for adipose organogenesis, and adult adipocytes fate map to a mural (smooth muscle actin-positive [SMA$^+$]) cell lineage (Jiang et al., 2014). It is possible that rosiglitazone and roscovitine activate the recruitment of PPARγ$^+$/SMA$^+$ progenitors to differentiate into brite adipocytes. Both beige and brite cells could arise from the same mural compartment of progenitors but have traveled down different pathways due to the nature of their regulators. Beige adipogenesis is likely stimulated by factors such as prostaglandin (Vegiopoulos et al., 2010) released from mature white adipocytes that express β-adrenergic receptors. Brite adipogenesis might be driven by stimulation of PPARγ in the mural cells with roscovitine. The possibility also exists that PPARγ stimulation could release browning factors from white adipocytes. These factors would likely be distinct from those released by CL316,243 because the resulting UCP1$^+$ adipocytes are different. It will be interesting to see whether brite cells can arise from a natural physiological stimulus as is the case with catecholamine induction of beige cells. It is conceivable that physiological effectors regulating the post-translational modification of PPARγ can influence the browning (brite cells) potential of WAT under different metabolic conditions. Our identification of selective markers for beige (i.e., Trim17) and brite (i.e., Gp×8) cells should aid in the classification of UCP1$^+$ adipocytes arising in response to different stimuli.

In conclusion, these studies have provided strong evidence for the recruitment of distinct types of UCP1$^+$ adipocytes in WAT by different browning agents. Beige adipocytes that arise from a population of progenitors expressing Tmem26 and CD137 can be recruited by cold exposure or treatment with β-adrenergic agonists. The brite adipocytes that form in response to roscovitine, as well as rosiglitazone, are similar to each other but distinct from beige adipocytes. It is not surprising that roscovitine gives rise to adipocytes similar to those arising from treatment with rosiglitazone, because the data strongly suggest that the former acts by stimulating PPARγ activity. When considering its therapeutic potential, however, roscovitine appears to generate a healthier metabolic profile than rosiglitazone. Both drugs protect mice from diet-induced glucose intolerance but roscovitine also enhances energy expenditure and lowers weight gain. Additionally, roscovitine unlike rosiglitazone or CL316,243, prevented diet-induced hepatic steatosis. It is very possible, therefore, that roscovitine will not be plagued by the life-threatening side effects associated with rosiglitazone therapy. Finally, just as recent studies have used markers of classic brown and beige adipocytes to classify adipocytes in the neck and thoracic regions of humans, it will be important to include the new set of markers for all UCP1$^+$ adipocytes as presented here.

EXPERIMENTAL PROCEDURES

Plasmids and Cell Lines

Replacement of S273 of PPARγ with alanine and establishment of Swiss 3T3 cell lines expressing WT- and S273A-PPARγ, as well as the growth and differentiation of 3T3 L1 preadipocytes and the PPARγ cell lines, were as previously described (Wang et al., 2008). Cells were treated with roscovitine (Cayman Chemical Company) and Troglitazone (Sigma) at the times described in the legends of Figures 1 and 2.

Antibodies and Western Blot Analysis

Total cellular protein and tissue samples were extracted and subjected to western blot analysis as described (Wang et al., 2008) using antibodies against adiponectin (Thermo Scientific), ERK (BD Bioscience), p-ERK (Cell Signaling), PPARγ (Santa Cruz), pS273 PPARγ (Bioss), pS112PPARg (Abcam), and UCP1 (Abcam).

Animals

C57BL/6N wild-type mice for experiments were obtained from Taconic. UCP1-Cre mice and B6.129(Cg)-Gt(ROSA)26Sortm4(ACTB-tdTomato,-EGFP)Luo/J (mTmG) mice are from Jackson Laboratory. The Ucp1-cre mice were crossed with mTmG mice to remove the flox-flanked resistance cassette. Mice were housed at 23°C in a 12 hr light/dark cycle with free access to normal chow. All experiments used matched littermates. Experimental procedures were approved by the Boston University Institutional Animal Care and Use Committee. For diet studies, 8-week-old C57BL/6N wild-type male mice were fed a diet with 60% kcal% fat (high fat diet, Research Diets, D12492) for 9 weeks. During the last 6 weeks of the diet, the mice were intraperitoneally (i.p.) injected daily with rosiglitazone (10 mg/kg), or roscovitine (50 mg/kg), or CL-316,243 (1 mg/kg), or vehicle. For cold exposure experiment, body temperatures were measured rectally using a digital thermometer.

Indirect Calorimetry and Body Composition

For determination of energy expenditure, mice were injected (i.p.) daily with rosiglitazone (10 mg/kg), or roscovitine (50 mg/kg), or CL-316,243 (1 mg/kg), or vehicle (−) for 6 weeks. Oxygen consumption, carbon dioxide production, RER, food intake, and physical activity were measured continuously using Comprehensive Laboratory Animal Monitoring System (CLAMS) consisting of open circuit calorimeter and motion detectors. Body composition was measured by noninvasive quantitative MRI (EchoMRI700).

Glucose Tolerance Tests and Serum Insulin

Mice were fasted for 6 hr, then blood glucose was measured (Bayer Contour) after tail bleeding at 0, 15, 30, 60, and 120 min following an injection of glucose (2 mg/kg body weight). Mice were euthanized, and serum obtained from heart blood using serum separation tubes (BD) was analyzed using mouse insulin ELISA kit (Crystal Chem).

Histology

Adipose tissues were excised, fixed in 10% formalin, paraffin-embedded, and sectioned (10-mm) prior to H&E staining or immunohistochemistry for UCP1 (Abcam; 1:100) detection. Signal was detected using the Vector ABC Elite kit.

Confocal Fluorescence Microscopy of Adipose Tissue and Adipocytes

Adipose tissues were excised, washed in PBS twice and cut into tiny pieces, and mounted on microscope slides (Fisherfinest). Adipocytes were washed three times with PBS and fixed with 3% (w/v) paraformaldehyde in PBS for 20 min at room temperature. Slides were prepared and imaged on the same day. Fluorescence micrographs were obtained using a Zeiss LSM 710-Live Duo scan at the Cellular Imaging Core at Boston University. Background was adjusted using samples from GFP^{-} and/or RFP^{-} littermates, and final images were intensity-adjusted using Zen software.

FACS of Adipocyte Subpopulations

Adipocytes were isolated by fractionation of collagenase-digested adipose tissue as outlined in detail in the Supplemental Experimental Procedures. Specialized adipocyte FACS strategy was developed at the BUSM Flow Cytometry Core Facility. The technical details will be available upon request.

Sorting of adipocytes was performed using a BD FACS Aria II high-speed sorter (BD Bioscience). A total of 40,000–160,000 living cells per adipocyte group were collected in lysis buffer of the RNeasy Plus Micro Kit (QIAGEN) and flash-frozen on dry ice.

RNA Extraction, cDNA Synthesis, and Quantitative Real-Time PCR

Total RNA was extracted from tissues or unsorted cells using Trizol reagent (Invitrogen) according to the manufacturer's instructions. RNA from sorted cells was prepared using the RNeasy Plus Micro Kit (QIAGEN). Reverse transcription of RNA from tissues or unsorted cells was performed using the High Capacity cDNA Reverse transcription kit (Applied Biosystems) with 2,000 ng of RNA. Amplification and reverse transcription of RNA from sorted cells was performed using Ambion WT expression kit (Affymetrix) with 50 ng of RNA. qPCR was performed on a ViiA 7 (Applied Biosystems), and relative mRNA concentrations, which were normalized to 36B4 RNA, were calculated by the ΔΔCt method.

Microarray Analyses of Adipose Tissue Cell Populations

All procedures were performed at the Boston University Microarray & Sequencing Resource Facility as described in the GeneChip Whole Transcript (WT) Pico Reagent Kit Manual (Affymetrix). Details are outlined in the Supplemental Experimental Procedures. Microarray data have been deposited in the GEO: GSE87191.

Statistics

All results are presented as mean ± SD. p values were calculated by unpaired Student's t test (*$p < 0.05$, **$p < 0.01$, and ***$p < 0.001$; $p < 0.05$ was considered significant throughout).

For cultured and primary isolated cells, all experiments were performed independently at least three times. Animal studies were from 4–6 animals per group.

Supplementary Material

Refer to Web version on PubMed Central for supplementary material.

Acknowledgments

We thank the members of the S.R.F. laboratory for helpful discussions. We thank Brian R. Tilton for specialized adipocyte FACS at BUSM Flow Cytometry Core Facility. We acknowledge Tom Balon of the Mouse Phenotyping/IVIS Core for his advice and assistance. This work was supported by NIH grants DK098830 (S.R.F.), DK102199 (S.R.F.), and T32DK007201 (J.Z.L.), a Pilot and Feasibility grant (P30 DK046200) from the Boston Nutrition Obesity Research Center (T.R.A.), and a CTSA grant (1UL1TR001430).

References

Banks AS, McAllister FE, Camporez JP, Zushin PJ, Jurczak MJ, Laznik-Bogoslavski D, Shulman GI, Gygi SP, Spiegelman BM. 2015; An ERK/Cdk5 axis controls the diabetogenic actions of PPARγ. Nature. 517:391–395. [PubMed: 25409143]

Cannon B, Nedergaard J. 2004; Brown adipose tissue: function and physiological significance. Physiol Rev. 84:277–359. [PubMed: 14715917]

Choi JH, Banks AS, Estall JL, Kajimura S, Boström P, Laznik D, Ruas JL, Chalmers MJ, Kamenecka TM, Blüher M, et al. 2010; Anti-diabetic drugs inhibit obesity-linked phosphorylation of PPARgamma by Cdk5. Nature. 466:451–456. [PubMed: 20651683]

Choi JH, Banks AS, Kamenecka TM, Busby SA, Chalmers MJ, Kumar N, Kuruvilla DS, Shin Y, He Y, Bruning JB, et al. 2011; Antidiabetic actions of a non-agonist PPARγ ligand blocking Cdk5-mediated phosphorylation. Nature. 477:477–481. [PubMed: 21892191]

Cinti S. 2005; Theadiposeorgan. Prostaglandins Leukot Essent Fatty Acids. 73:9–15. [PubMed: 15936182]

Cinti S. 2012; The adipose organ at a glance. Dis Model Mech. 5:588–594. [PubMed: 22915020]

Deng Y, Scherer PE. 2010; Adipokines as novel biomarkers and regulators of the metabolic syndrome. Ann N Y Acad Sci. 1212:E1–E19.

Farmer SR. 2009; Obesity: be cool, lose weight. Nature. 458:839–840. [PubMed: 19370020]

Giordano A, Smorlesi A, Frontini A, Barbatelli G, Cinti S. 2014; White, brown and pink adipocytes: the extraordinary plasticity of the adipose organ. Eur J Endocrinol. 170:R159–R171. [PubMed: 24468979]

Jiang Y, Berry DC, Tang W, Graff JM. 2014; Independent stem cell lineages regulate adipose organogenesis and adipose homeostasis. Cell Rep. 9:1007–1022. [PubMed: 25437556]

Liu J, Wang H, Zuo Y, Farmer SR. 2006; Functional interaction between peroxisome proliferator-activated receptor gamma and beta-catenin. Mol Cell Biol. 26:5827–5837. [PubMed: 16847334]

Long JZ, Svensson KJ, Tsai L, Zeng X, Roh HC, Kong X, Rao RR, Lou J, Lokurkar I, Baur W, et al. 2014; A smooth muscle-like origin for beige adipocytes. Cell Metab. 19:810–820. [PubMed: 24709624]

Nolte RT, Wisely GB, Westin S, Cobb JE, Lambert MH, Kurokawa R, Rosenfeld MG, Willson TM, Glass CK, Milburn MV. 1998; Ligand binding and co-activator assembly of the peroxisome proliferator-activated receptor-gamma. Nature. 395:137–143. [PubMed: 9744270]

Pascual G, Fong AL, Ogawa S, Gamliel A, Li AC, Perissi V, Rose DW, Willson TM, Rosenfeld MG, Glass CK. 2005; ASUMOylation-dependent pathway mediates transrepression of inflammatory response genes by PPAR-gamma. Nature. 437:759–763. [PubMed: 16127449]

Petrovic N, Walden TB, Shabalina IG, Timmons JA, Cannon B, Nedergaard J. 2010; Chronic peroxisome proliferator-activated receptor gamma (PPARgamma) activation of epididymally derived white adipocyte cultures reveals a population of thermogenically competent, UCP1-

containing adipocytes molecularly distinct from classic brown adipocytes. J Biol Chem. 285:7153–7164. [PubMed: 20028987]

Qiang L, Wang L, Kon N, Zhao W, Lee S, Zhang Y, Rosenbaum M, Zhao Y, Gu W, Farmer SR, Accili D. 2012; Brown remodeling of white adipose tissue by SirT1-dependent deacetylation of Pparγ. Cell. 150:620–632. [PubMed: 22863012]

Rull A, Geeraert B, Aragonès G, Beltrán-Debón R, Rodríguez-Gallego E, García-Heredia A, Pedro-Botet J, Joven J, Holvoet P, Camps J. 2014; Rosiglitazone and fenofibrate exacerbate liver steatosis in a mouse model of obesity and hyperlipidemia. A transcriptomic and metabolomic study. J Proteome Res. 13:1731–1743. [PubMed: 24479691]

Sun K, Kusminski CM, Scherer PE. 2011; Adiposetissue remodeling and obesity. J Clin Invest. 121:2094–2101. [PubMed: 21633177]

Vegiopoulos A, Müller-Decker K, Strzoda D, Schmitt I, Chichelnitskiy E, Ostertag A, Berriel Diaz M, Rozman J, Hrabe de Angelis M, Nüsing RM, et al. 2010; Cyclooxygenase-2 controls energy homeostasis in mice by de novo recruitment of brown adipocytes. Science. 328:1158–1161. [PubMed: 20448152]

Vernochet C, Peres SB, Davis KE, McDonald ME, Qiang L, Wang H, Scherer PE, Farmer SR. 2009; C/EBPalpha and the corepressors CtBP1 and CtBP2 regulate repression of select visceral white adipose genes during induction of the brown phenotype in white adipocytes by peroxisome proliferator-activated receptor gamma agonists. Mol Cell Biol. 29:4714–4728. [PubMed: 19564408]

Wang H, Qiang L, Farmer SR. 2008; Identification of a domain within peroxisome proliferator-activated receptor gamma regulating expression of a group of genes containing fibroblast growth factor 21 that are selectively repressed by SIRT1 in adipocytes. Mol Cell Biol. 28:188–200. [PubMed: 17954559]

Wu J, Boström P, Sparks LM, Ye L, Choi JH, Giang AH, Khandekar M, Virtanen KA, Nuutila P, Schaart G, et al. 2012; Beige adipocytes are a distinct type of thermogenic fat cell in mouse and human. Cell. 150:366–376. [PubMed: 22796012]

Highlights

- Roscovitine inhibits phosphorylation of S273 of PPARγ and induces brown adipocyte genes
- Roscovitine browns white fat and enhances energy expenditure
- FACS enrichment of UCP1^{+} adipocytes enables molecular profiling
- Roscovitine-induced UCP1^{+} adipocytes are distinct from beige adipocytes

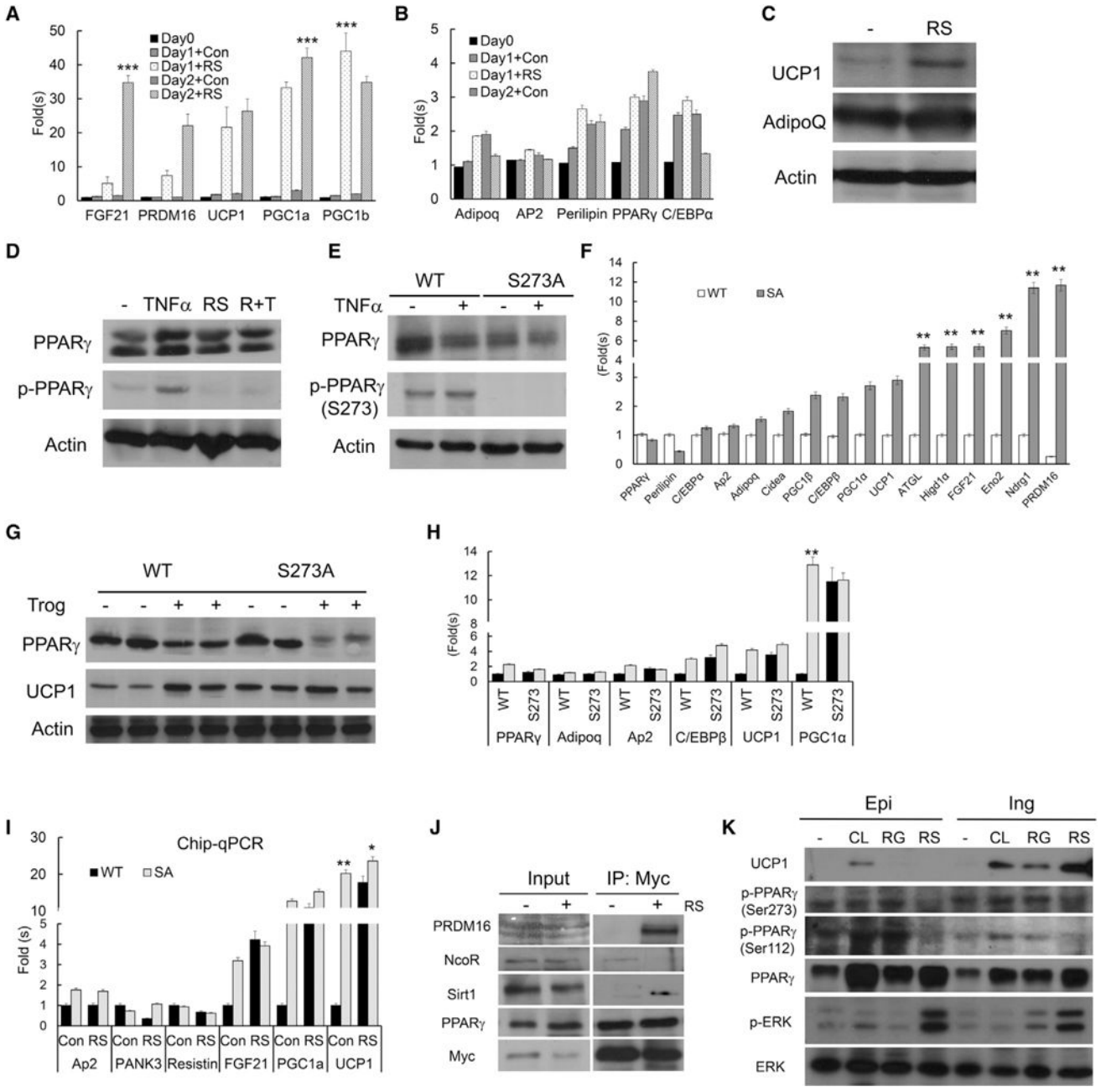

Figure 1. Roscovitine Enhances Brown Gene Expression in Mature Adipocytes by Inhibiting Phosphorylation of S273 of PPARγ

(A) Treatment of 3T3-L1 adipocytes with roscovitine (5 μm) for 1–2 days induced select brown adipocyte mRNAs.

(B) Treatment of 3T3-L1 adipocytes with roscovitine (5 μm) for 1–2 days had no effect on white adipocyte mRNAs.

(C) Two days of exposure of 3T3-L1 adipocytes to roscovitine increases UCP1 protein expression.

(D) Treatment of 3T3-L1 adipocytes for 1 hr with TNFα, roscovitine (RS), or TNFα with roscovitine (R+T).

(E) Western blot of proteins from Swiss WT-PPARγ and S273A-PPARγ adipocytes with or without TNFα.
(F) qPCR analysis of RNA from Swiss WT-PPARγ and S273A-PPARγ adipocytes.
(G) Western blot of proteins from Swiss WT-PPARγ and S273A-PPARγ induced to differentiate into adipocytes with or without troglitazone (5 mm).
(H) qPCR of RNA from Swiss WT-PPARγ and S273A-PPARγ cells induced to adipocytes with (gray) or without (black) roscovitine (5 μM).
(I) Roscovitine (RS) and S273A (SA) selectively enhance the binding of PPARγ to brown gene promoters.
(J) Roscovitine (RS) enhances the association of a Myc-tagged PPARγ with Sirt1 and PRDM16.
(K) Western blot of proteins from Epi and Ing WAT depots of 8-week-old C57BL/6Nwild-type male mice that were intraperitoneally (i.p.) injected dailyfor2weeks with vehicle (−), CL316,243 (CL), rosiglitazone (RG), or roscovitine (RS).
See also Figure S1.

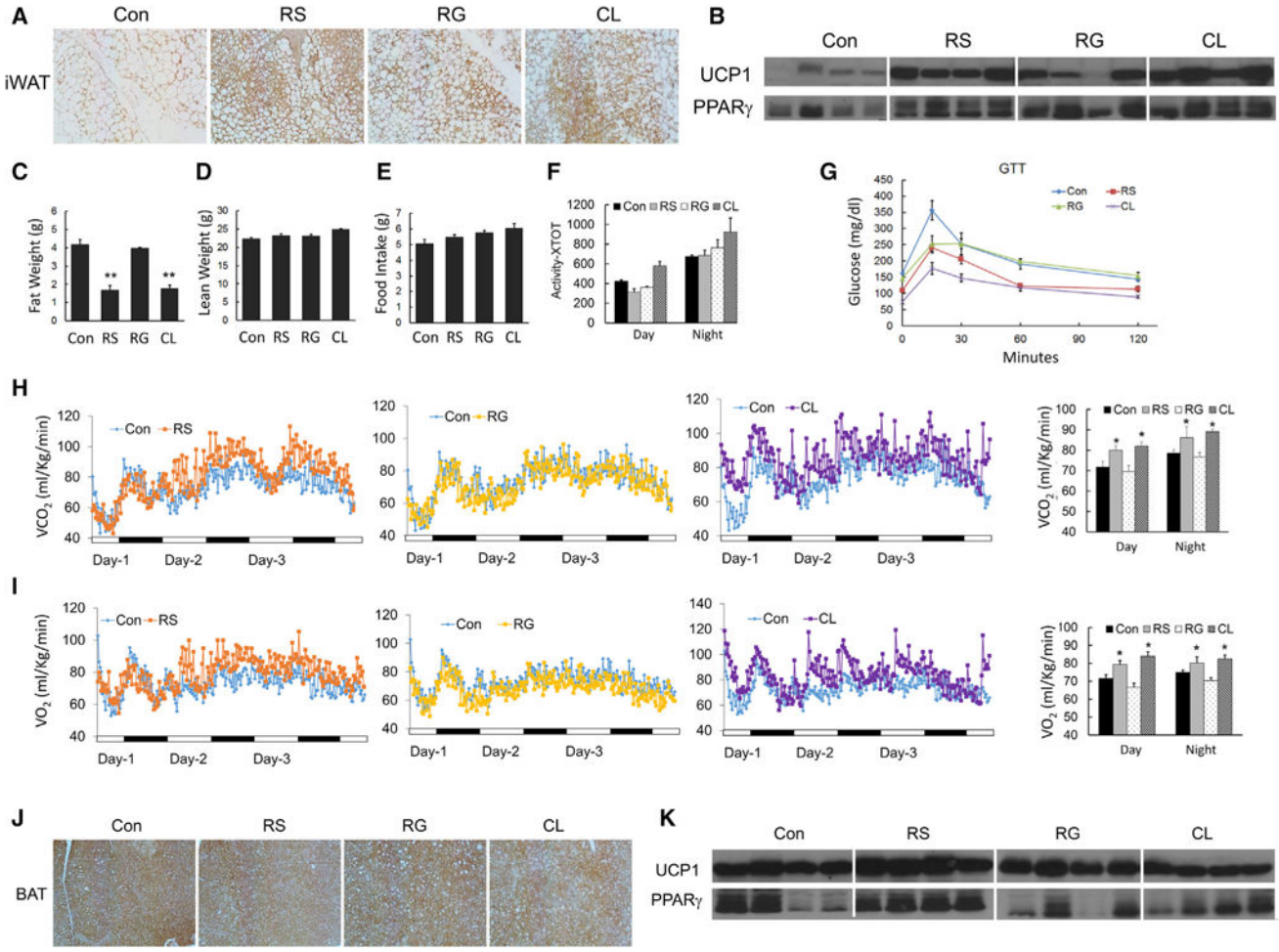

Figure 2. Roscovitine Induces Browning of IngWAT and Enhances Energy Expenditure in Mice

(A) UCP1 staining of sections of IngWAT depots from 8-week-old C57BL/6N wild-type male mice intraperitoneally (i.p.) injected daily for 6 weeks with roscovitine-RS (50 mg/kg), or rosiglitazone-RG (10 mg/kg), or CL-316,243 (1 mg/kg), or vehicle (−), n = 4/group.

(B) Expression of UCP1 protein in the same IngWAT depots analyzed in (A).

(C) Fat weight determined by nuclear magnetic resonance (NMR) (described in the Experimental Procedures) of mice from (A).

(D) Lean weight determined by NMR of mice from (A).

(E) Food intake of mice from (A).

(F) Physical activity measured by CLAMS.

(G) After 6 weeks of administration of drugs listed in (A), mice were then i.p. injected with glucose at 2 mg/kg of body weight after fasting 6 hr and whole-blood glucose was measured at 15, 30, 60, and 120 min.

(H and I) Mice from (A)were housed individually in metabolicchambersfor4daysand 3 nights. Traces of O_2 consumption (I) and CO_2 production (H) during 12 hr light anddark cycles measured by CLAMS.

(J) UCP1 staining of sections of BAT depots of mice from (A).

(K) Expression of UCP1 protein in the same BAT depots as (J).

See also Figure S2.

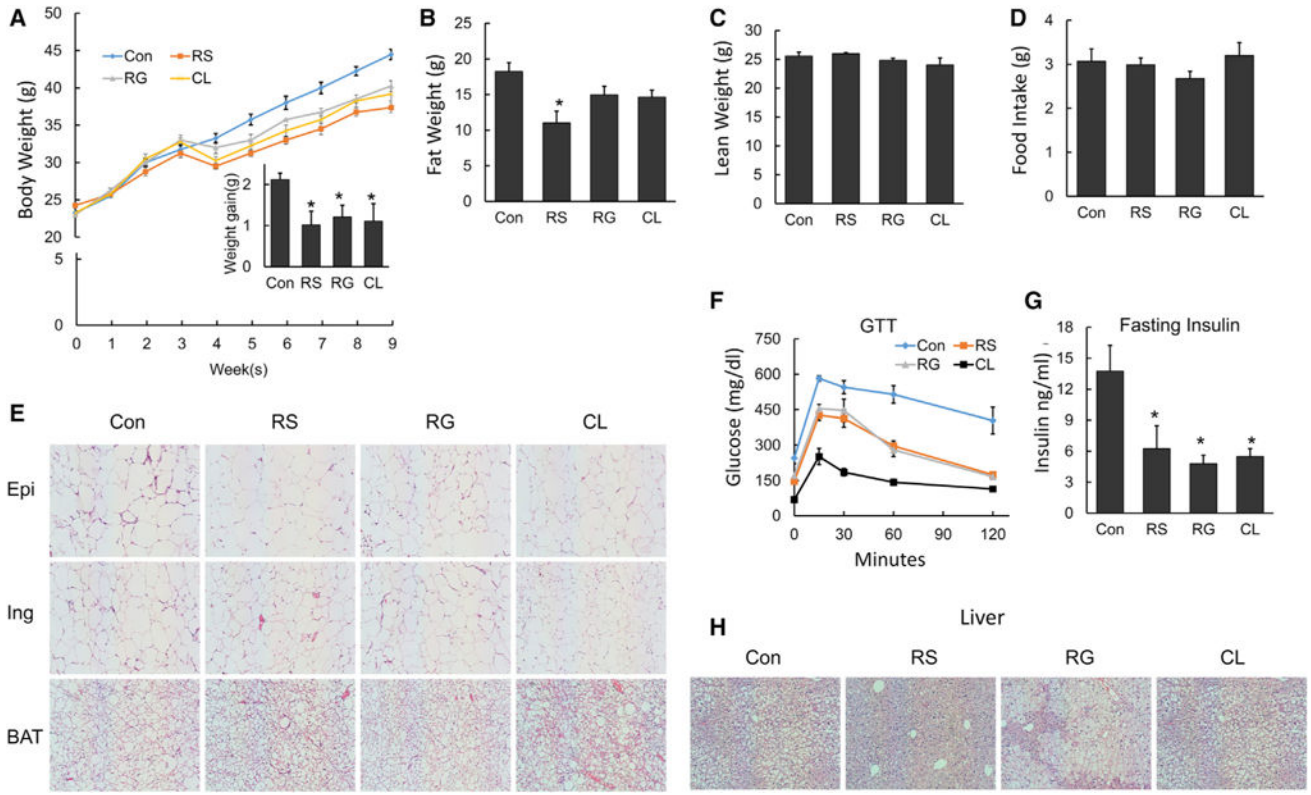

Figure 3. Roscovitine Protects against Diet-Induced Obesity and Glucose Intolerance

(A) Six-week-old mice were fed a rodent HFD (60% Kcal% fat) for 9 weeks. Three weeks into the diet, mice were i.p. injected with rosiglitazone (10 mg/kg), or roscovitine (50 mg/kg), or CL-316,243 (1 mg/kg) for 6 weeks. Body weight and weight gain were measured at weekly intervals, n = 4/group.

(B) Fat weight determined by NMR.

(C) Lean weight determined by NMR.

(D) Food intake was measured every 24 hr.

(E) H&E staining of sections of ING, EPI, and BAT depots from mice in (A) sacrificed at 9 weeks of diet.

(F) After 6 weeks drug treatment, mice were then i.p. injected with glucose at 2 mg/kg of body weight after fasting 6 hrand whole-blood glucose was measured at 15, 30, 60, and 120 min.

(G) Fasting blood insulin of mice after 9 weeks of HFD.

(H) H&E staining of sections of livers from mice in (E).

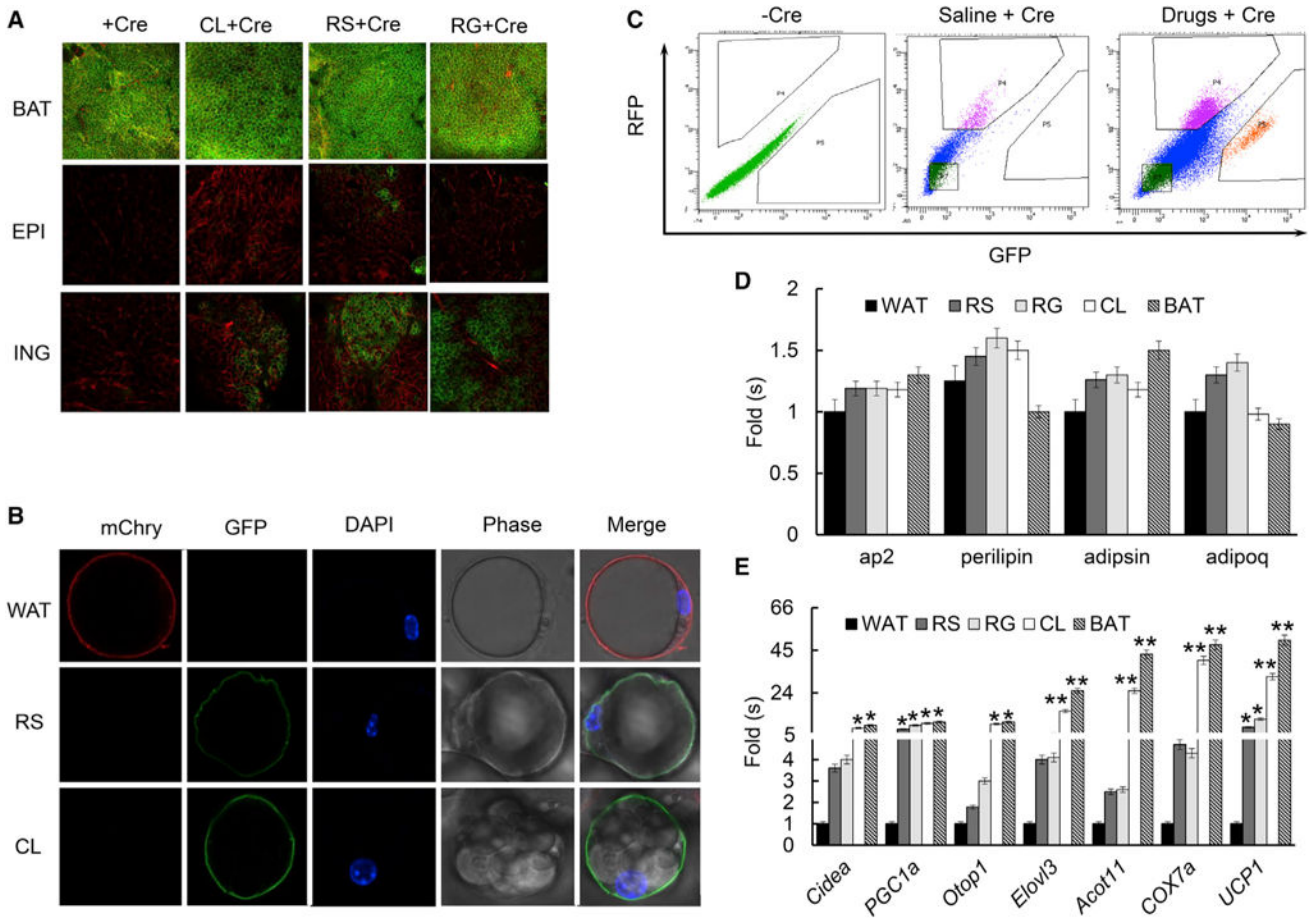

Figure 4. Fluorescence-Activated Cell Sorting of UCP1^{+} Adipocytes from ING Depots of Mice Treated with Different Browning Agents

(A) Confocal fluorescence images of ING, EPI, and BAT depots of 8-week-old UCPI-cre/Tomato mice injected daily for 2 weeks with CL-316,243 (CL), or roscovitine (RS), or rosiglitazone (RG) as in Figure 2A.

(B) Confocal microscopy of single cells in adipocyte suspensions prepared from ING depots of mice injected daily for 2 weeks with vehicle (WAT), CL-316,243 (CL), or roscovitine (RS).

(C) Representative FACS collection gates for the isolation of UCP1^{+} adipocytes (GFP) from adipose depots of 8-week-old UCP1-cre/Tomato mice injected daily for 2 weeks with vehicle or drugs as in (A).

(D) qPCR analysis of select adipogenic mRNAs expressed in WAT (RFP) and RS, RG, CL, and BAT (GFP) adipocytes isolated by FACS from ING depot as in (C).

(E) qPCR analysis of select brown marker mRNAs expressed inWAT (RFP) and RS, RG, CL, and BAT (GFP) adipocytes isolated by FACS from ING depot as in (C). See also Figure S3.

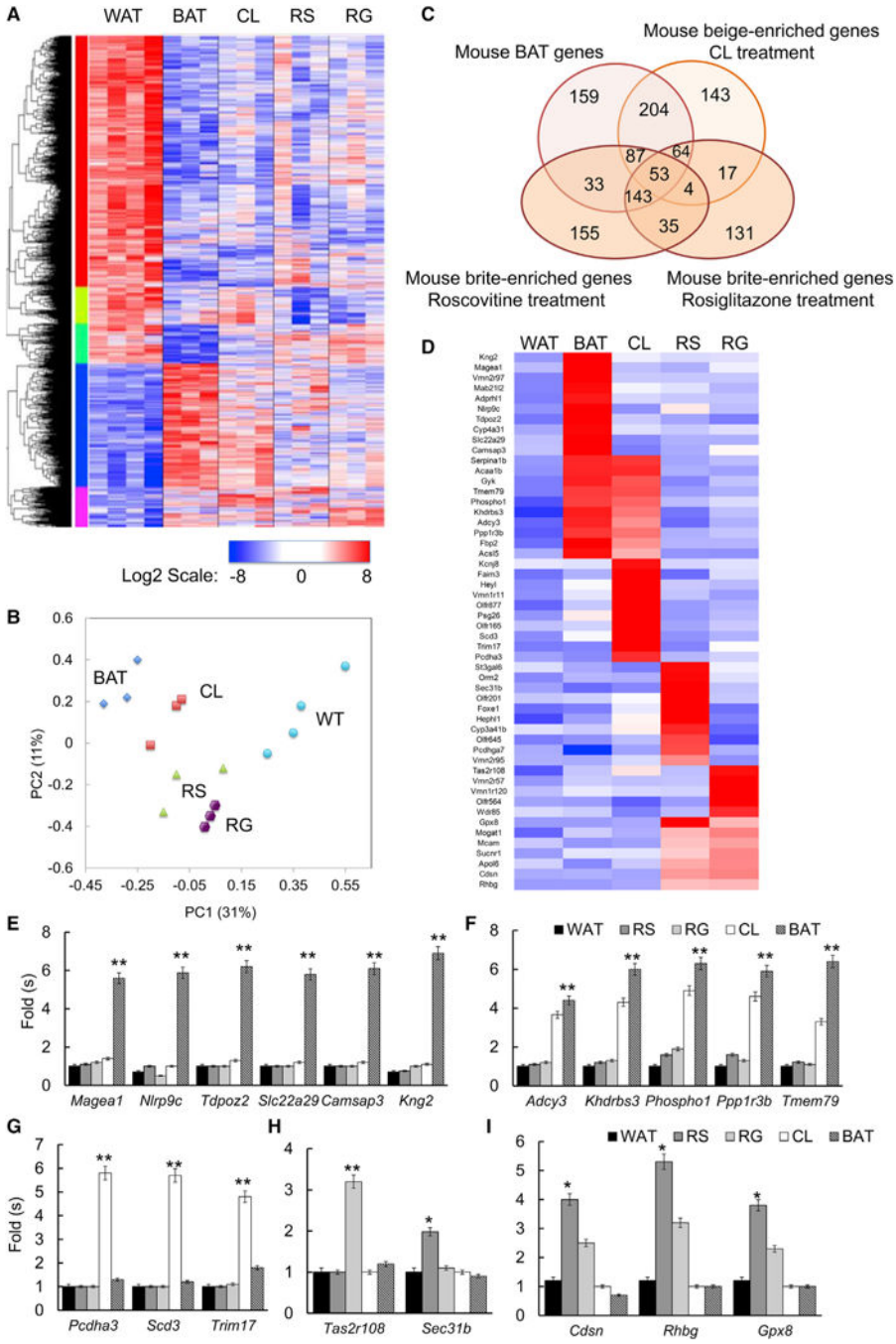

Figure 5. Genome-wide mRNA Expression Analyses Identify Distinct Populations of UCP1^{+} Adipocytes in ING WAT of Mice Treated with Different Browning Agents

(A) Heatmaps of microarrays corresponding to RNA from WAT, BAT, CL, RS, and RG adipocytes isolated as in Figure 4, n = 3–4/group.

(B) Principle component (PC) analysis of the transcriptome of adipocytes as identified in (A).

(C) The overlapping genes enriched by 2-fold or more in mouse classical brown adipocytes, mouse beige (CL) or brite adipocytes (RS and RG) versus white adipocytes.

(D) Heatmap of select genes enriched in each population of adipocytes (WAT, BAT, CL, RS, and RG).

(E–I) qPCR analysis of select genes expressed in the different adipocyte types. In each case, cells were isolated by FACS to enrich for RFP^+ (WAT) or GFP^+ (CL, RS, RG, and BAT) adipocytes. Genes enriched in: BAT (E); CL and BAT cells (F); CL cells (G); RS or RG cells (H); and RS and RG cells (I).

See also Figure S4.

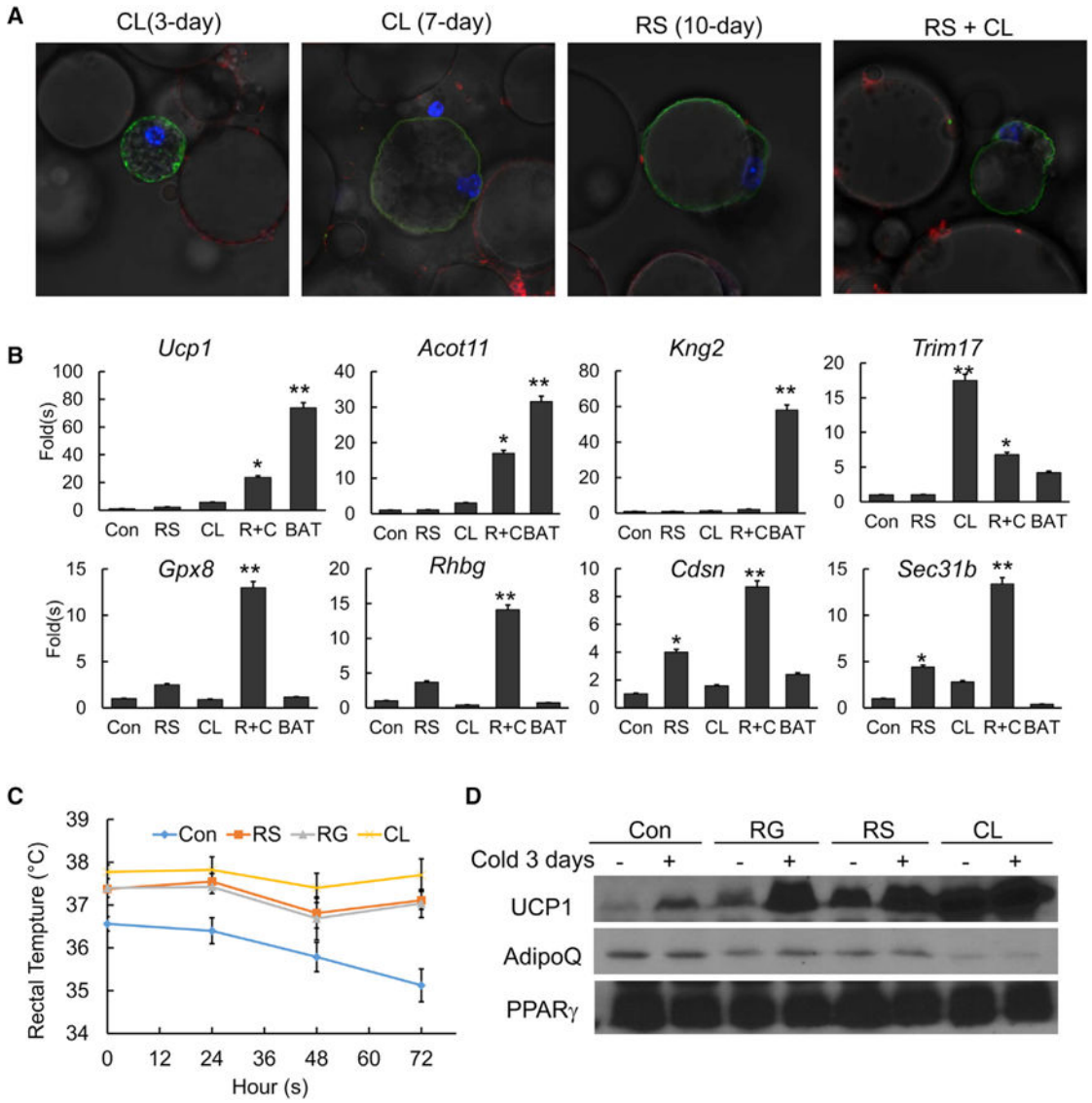

Figure 6. Roscovitine Induces Formation of a Unique Population of Thermogenic Adipocytes

(A) Confocal images of single adipocytes from UCPI-Cre/Tomato mice treated with CL316,243 (CL) for 3 or 7 days or with roscovitine for 10 days (RS) alone or followed by CL316,243 for 3 days (RS+CL).

(B) qPCR analysis of genes expressed in FACS isolated adipocytes from (A) (RS, CL, R+C) as well as from WAT (Con) and BAT.

(C) Mice were treated with CL, or RG, or RS, or vehicle for 10 days at which stage they were housed for 3 days in a cold room. Rectal temperature of control and treated mice was measured at outset and every 24 hr in cold room. n = 4/group.

(D) Proteins from drug-treated mice in (C) with and without exposure to cold were analyzed by western blot.